Journal of Volcanology and Geothermal Research xxx (2015) xxx–xxx

Contents lists available at ScienceDirect

Journal of Volcanology and Geothermal Research

journal homepage: www.elsevier.com/locate/jvolgeores

Magma migration at the onset of the 2012–13 Tolbachik eruption revealed by Seismic Amplitude Ratio Analysis

Corentin Caudron [a,*], Benoit Taisne [a,c], Yulia Kugaenko [b], Vadim Saltykov [b]

[a] Earth Observatory of Singapore, Nanyang Technological University, 50 Nanyang Avenue, Block N2-01a-15, 639798, Singapore
[b] Geophysical Survey of Russian Academy of Sciences, Kamchatka Branch, Petropavlovsk-Kamchatsky, Russian Federation
[c] Asian School of the Environment, Nanyang Technological University, 50 Nanyang Avenue, Block N2-01a-15, 639798, Singapore

ARTICLE INFO

Article history:
Received 15 February 2015
Accepted 2 September 2015
Available online xxxx

Keywords:
The 2012–13 Tolbachik eruption
Monitoring
Magma migration
Seismic Amplitude Ratio Analysis
Fissure eruption

ABSTRACT

In contrast of the 1975–76 Tolbachik eruption, the 2012–13 Tolbachik eruption was not preceded by any striking change in seismic activity. By processing the Klyuchevskoy volcano group seismic data with the Seismic Amplitude Ratio Analysis (SARA) method, we gain insights into the dynamics of magma movement prior to this important eruption. A clear seismic migration within the seismic swarm, started 20 hours before the reported eruption onset (05:15 UTC, 26 November 2012). This migration proceeded in different phases and ended when eruptive tremor, corresponding to lava flows, was recorded (at ~11:00 UTC, 27 November 2012). In order to get a first order approximation of the magma location, we compare the calculated seismic intensity ratios with the theoretical ones. As expected, the observations suggest that the seismicity migrated toward the eruption location. However, we explain the pre-eruptive observed ratios by a vertical migration under the northern slope of Plosky Tolbachik volcano followed by a lateral migration toward the eruptive vents. Another migration is also captured by this technique and coincides with a seismic swarm that started 16–20 km to the south of Plosky Tolbachik at 20:31 UTC on November 28 and lasted for more than 2 days. This seismic swarm is very similar to the seismicity preceding the 1975–76 Tolbachik eruption and can be considered as a possible aborted eruption.

1. Introduction

Nearly 36 years after its last eruption, the largest basaltic eruption in Kamchatka during historic times (the 1975–76 Tolbachik eruption), Tolbachik (Fig. 1) began erupting on 27 November 2012. While the 1975–76 Tolbachik eruption could be predicted one week in advance based on strong seismic precursors, the 2012–13 Tolbachik eruption was preceded by much weaker seismicity. Visual observations confirmed the onset of the eruption around 10 PM (local time) on 27 November 2012. Hence, a lack of information exists concerning the hours preceding this significant eruption.

Taisne et al. (2011) recently imaged the complex dike propagation dynamics during the January 2010 Piton de la Fournaise eruption (La Reunion, France) using a novel and simple method named Seismic Amplitude Ratio Analysis (SARA). The technique computes the ratios of seismic intensity recorded at different seismic stations which are thus independent of the seismic energy radiated at the source. Since drastic changes in attenuation are unlikely to occur at the time scale of magma intrusion, temporal evolutions in the measured ratio have to be explained by a change in the source location. This study investigates the seismicity recorded during the days preceding and following the onset of the 2012–13 Tolbachik eruption using this simple approach.

2. Volcanic settings

Tolbachik volcanic zone, situated in the south part of Klyuchevskoy volcano group in Kamchatka, is a cluster of basaltic eruptive centers of different ages (Fig. 1). It includes the Pleistocene-aged Ostry Tolbachik and Plosky Tolbachik stratovolcanoes, as well as numerous Holocene-aged monogenetic cinder cones and vents located along rift zones to the NE and SSW of the main massif (Fig. 1). For the purpose of this paper, the Tolbachik Volcanic Zone is referred to as Tolbachik.

One of the features of Ostry and Plosky Tolbachik volcanoes is the well developed dike complex. The 1 to 10 m thick dikes on their slopes corresponds to radial and ring structures with lengths reaching 1.5 to 2 km. Geochemical and petrological investigations have shown different rock compositions ranging from basaltic to basaltic andesitic and corresponding to stratovolcano and monogenic volcanic field rocks (Churikova et al., 2015, in this issue). Additionally, in some cases, mixing of various melts was detected. Dikes on the slopes of Ostry and Plosky Tolbachik volcanoes appear as feeding channels for Late-Pleistocene–Holocene eruptions (Churikova et al., 2015, in this issue).

* Corresponding author.
E-mail address: CCaudron@ntu.edu.sg (C. Caudron).

http://dx.doi.org/10.1016/j.jvolgeores.2015.09.010

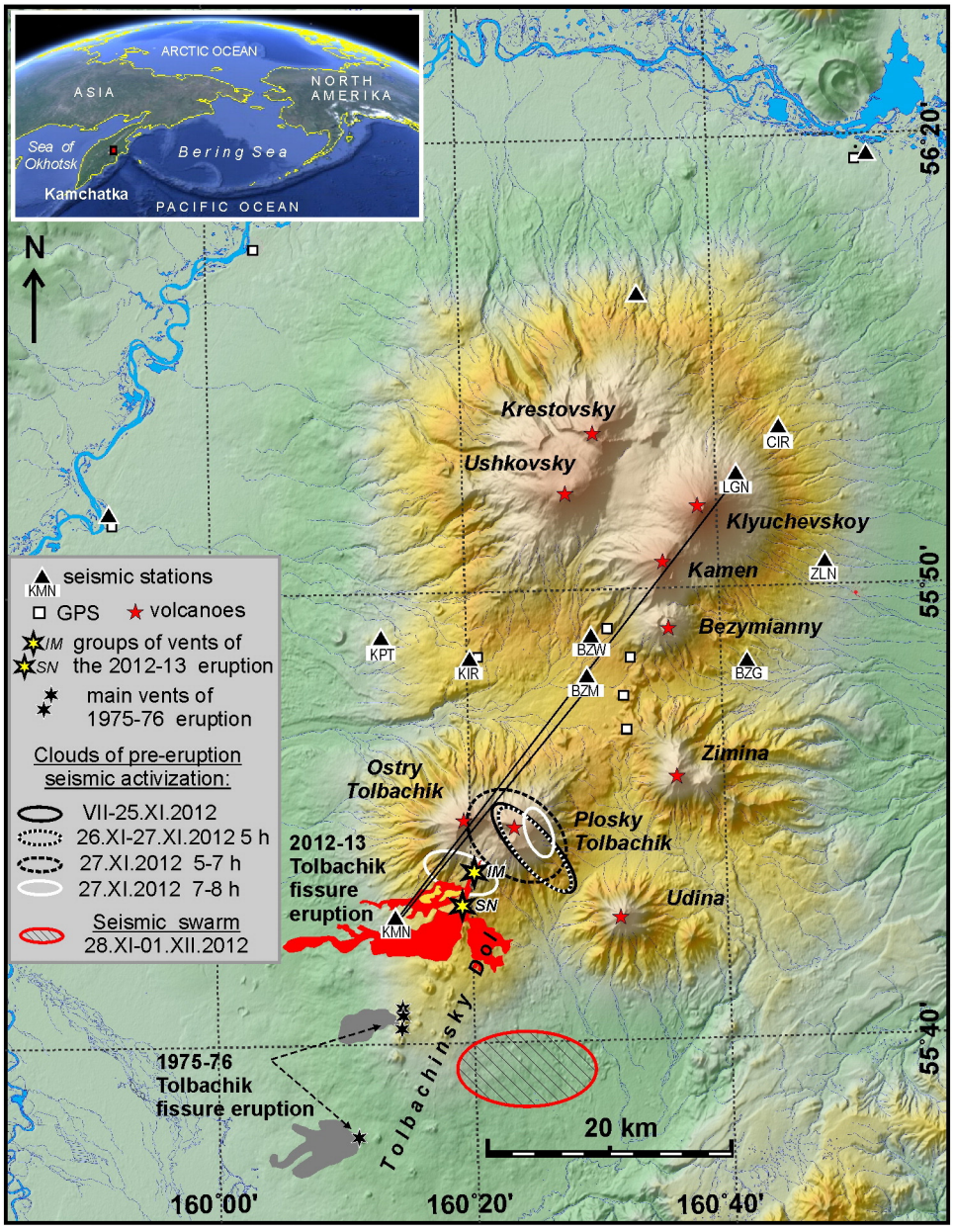

Fig. 1. Network: Map of Klyuchevskoy volcano group and its seismic monitoring network (Chebrov et al., 2013) (black triangles). Seismic data are transmitted to the Processing Center in real time by radio-telemetric system. Observations are carried out by Kamchatkan Branch of Geophysical Survey of Russian Academy of Sciences. The nearest GPS sites (white squares) are located at a distance of ~20–25 km to the north the 2012–2013 Tolbachik eruption area. Black lines indicate the station pairs used in this study.

The SSW rift zone is the most active area of Tolbachik during the last 2,000 years. It is named as Tolbachinsky Dol and is famous due to the 1975–76 Tolbachik eruption, when during ~18 months, more than 1 km^3 of magma was erupted. The 1975–76 Tolbachik eruption was predicted due to the intensive seismicity (M = 2–5) that began 9 days prior to the eruption. Its eruptive products included high-magnesium basalts that were interpreted to be sourced from depths larger than 20 km, as well as high-aluminum basalts that were likely sourced from a shallow magma reservoir beneath Plosky Tolbachik (Fedotov & Markhinin, 1983).

3. Chronology of the eruption

After 37 years of quiescence, on 27 November 2012, a renewed activity at Tolbachik began at the southern slope of Plosky Tolbachik volcano (Fig. 1). The new fissure eruption which was dominantly effusive, lasted until September 2013 and erupted approximately 0.55 km^3 of magma (Belousov et al., 2015, in this issue). The activity was located in the northern part of the SSW rift (Fig. 1).

The appearance of a radial linear fissure on the volcano slope with the subsequent formation of a chain of eruptive craters along it is a general pattern for the dynamics of flank eruptions at stratovolcanoes (Fedotov et al., 1991). The upper craters are mainly explosive, the lower ones are explosive–effusive or effusive; one of the lower craters is, as a rule, replaced by a cinder cone from which a lava flow pours out. However, during the initial stages of the 2012–13 Tolbachik eruption, the lava discharge from the upper part was much more intensive than the explosive activity. It started from a ~6 km long radial fissure, on the SW slope of Plosky Tolbachik (Fig. 1), opening at 2358 m to 1460 m a.s.l. (Dvigalo et al., 2014). Two groups of eruptive centers were formed on the fissure at the eruption onset and were named after two well-known Kamchatka volcanologists: the upper group after Igor Menyailov (the IM Vent, h = 1850 m) and the lower group after Sofia Naboko (the SN Vent, h = 1740 m). The SN Vent formed

Please cite this article as: Caudron, C., et al., Magma migration at the onset of the 2012–13 Tolbachik eruption revealed by Seismic Amplitude Ratio Analysis, J. Volcanol. Geotherm. Res. (2015), http://dx.doi.org/10.1016/j.jvolgeores.2015.09.010

later than the IM Vent. The opening of both eruptive centers was characterized by explosive activity with ash falls reported to distances up to 50 km from Tolbachik volcano (Melnikov & Volynets, 2015 in this issue).

Using joint satellite (ash clouds trajectories, SO_2 concentrations, meteorological conditions of the first days of eruption) and petrological data (alkalis, MgO content, K_2O/MgO ratio), (Melnikov & Volynets, 2015 in this issue) estimated the time of the SN Vent opening to be after 2:00 UTC on November 28. Morphologically, lava flows at this period were dominantly aa-lava type, but lava erupted from IM Vent presented higher silica and alkalis concentrations, and lower MgO content. That may be caused by the discharge of two levels of the magma chamber, fractionated to a different extent (Volynets et al., 2013). During the first two days of eruption, the lava discharge rate was very high (~440 m^3/s (Dvigalo et al., 2014)) and lava fields from the IM and SN Vents covered an area of ~14.4 km^2 (Dvigalo et al., 2014). The microstructures and textures of the lava produced at the beginning of the eruption suggest a very rapid supply of magma to the surface (Volynets et al., 2013). The IM Vent was active during the first three days of eruption only. After December 1, effusive activity became concentrated at the SN Vent. Additional general information concerning this eruption can be found in Belousov et al. (2015, in this issue) and Churikova et al. (2015, in this issue).

Contrary to the 1975–76 Tolbachik eruption, the 2012–13 eruption was not preceded by intensive seismic activity. For earthquake locations, a one-dimensional empirical model is used (Senyukov, 2006). For the Tolbachik volcano area, the level of reliable recordings of earthquakes (magnitude of completeness) is M = 1.3. The detection threshold is approximately M = 0.7. The mean error on locations for the 2010–2012 earthquakes are 3.0 ± 1.5 km in the horizontal directions and 3 ± 1 km in depth (Kugaenko et al., 2015, in this issue). The analysis of the 2000–2012 Tolbachik seismic catalogue showed an increase in low-energy seismicity (M = 1.2–2.3) occurring in July–November 2012, less than 5 km below Plosky Tolbachik volcano (Fig. 2). The inferred locations of the earthquake hypocenters were very stable during this time (Fig. 2). The seismic pattern abruptly changed on November 27 during the few hours preceding eruption with an increase of larger magnitude earthquakes (M = 3–4) (Edwards et al., 2013; Kugaenko et al., 2015, in this issue). This seismic activation may be interpreted as a magma ascent from a crustal magma chamber.

4. Methodology and results

In 2012, the seismic network at the Klyuchevskoy volcano group consisted of 12 seismic stations (Fig. 1) with real time radio-telemetric transmission to the Data Processing Centre in Petropavlovsk-Kamchatsky. All stations were equipped with 3-components short-period seismometers SM-3 (T = 1.2 second). We first check for the quality of the data by looking at seismic waveforms (Fig. 3a,c,e and supplementary material) and computing spectrograms (Fig. 3b,d,f and

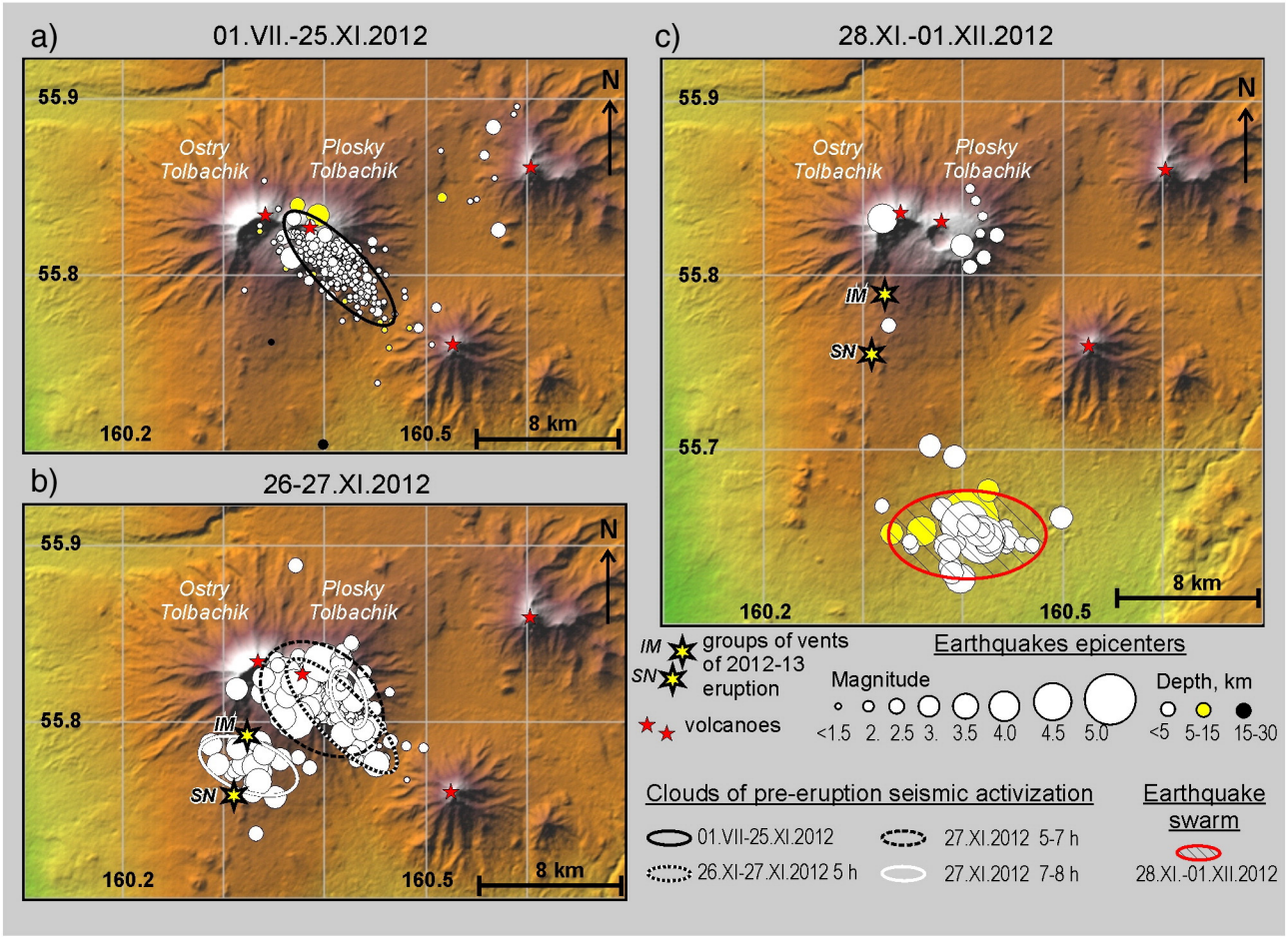

Fig. 2. Seismicity: Location and characteristics of the seismicity recorded before and during the volcanic eruption onset. Legend shows earthquakes epicenters grouped by depth (different colors) and sized by magnitude. Ellipses are drawn for reference: the spatial position of earthquake epicenters is described by a 2D Gaussian distribution, and ellipses include 90% of the events of the earthquakes clouds. Epicenters for small earthquakes (M < 1.5) are present in Fig. 2B, but are overlapped by stronger seismic events which occurred on November 27. Small earthquakes are absent in the catalogue and in Fig. 2C due to intense volcanic tremor. (For interpretation of the references to color in this figure legend, the reader is referred to the web version of this article.)

Please cite this article as: Caudron, C., et al., Magma migration at the onset of the 2012–13 Tolbachik eruption revealed by Seismic Amplitude Ratio Analysis, J. Volcanol. Geotherm. Res. (2015), http://dx.doi.org/10.1016/j.jvolgeores.2015.09.010

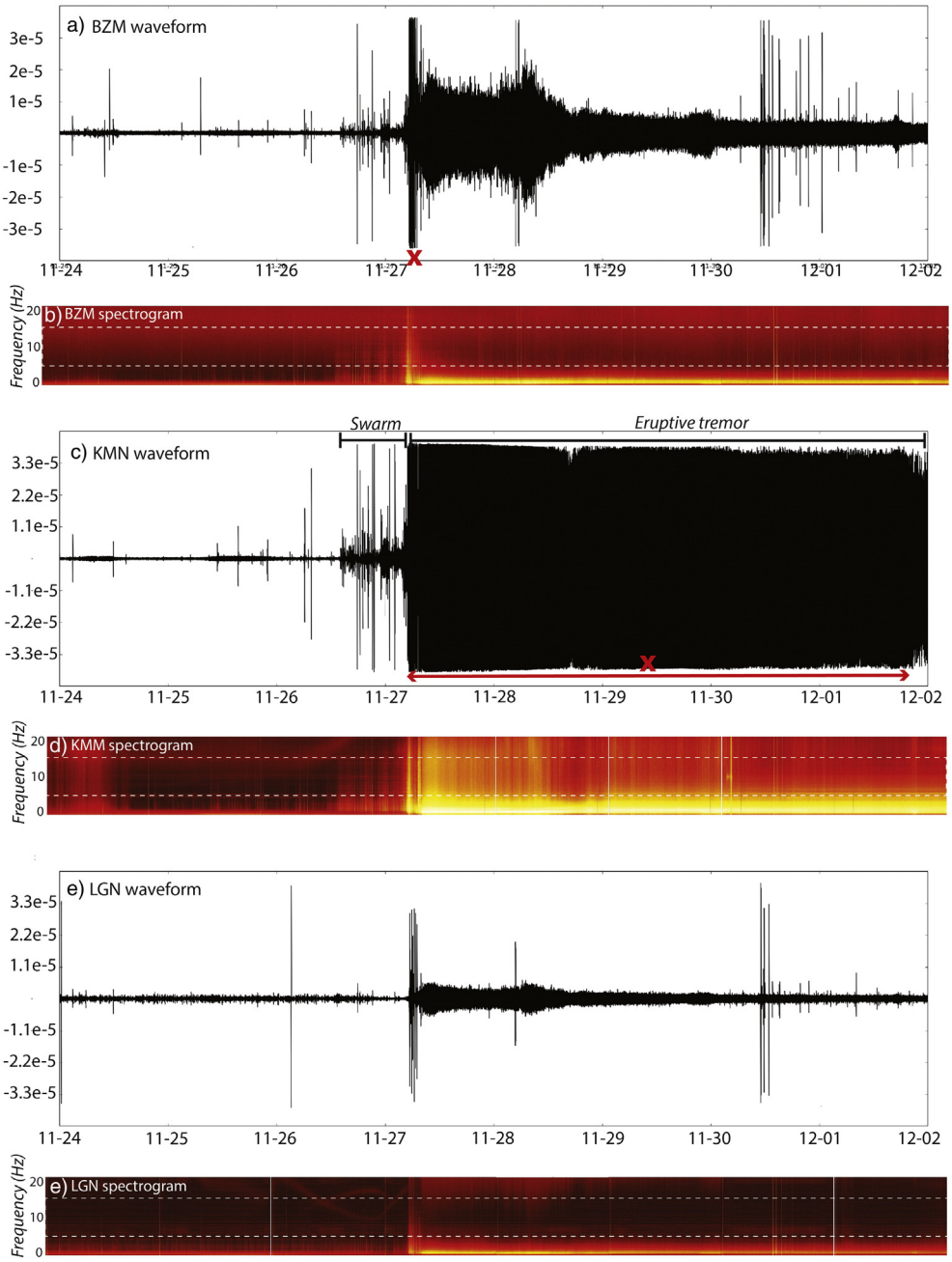

Fig. 3. Waveforms and spectrograms: Waveforms and spectrograms of the stations used in this study. Waveforms are downsampled to 32 Hz. Spectrograms are computed from the raw data, demeaned and cosine tapered (10%) beforehand, using a 4096 samples window with an overlap of 2000 samples. (a) and (b) correspond to BZM station; (c) and (d) to KMN; (e) and (f) to LGN stations (see Fig. 1 for station locations). White dashed rectangles on (b), (d), and (f) indicate the frequency band used for Seismic Amplitude Ratio calculations. We indicate the main swarm and eruptive tremor recorded at KMN on (c). Periods of clipped data are indicated using a red cross on (a) and (c). (For interpretation of the references to color in this figure legend, the reader is referred to the web version of this article.)

supplementary material). KMN station (Fig. 3c,d) is the only seismic station located nearby Tolbachik volcano (Fig. 1) and consequently constitutes our station of reference. Following the computations of waveforms and spectra for each seismic station, we decided to use also BZM (Fig. 3a,b), located around Bezymianny volcano, 25 km to the north of KMN station (Fig. 1), and LGN (Fig. 3e,f) nearby Klyuchevskoy volcano, situated at 45 km to the north of KMN station (Fig. 1). These stations are less noisy than others in the 5–15 Hz frequency band (white dashed rectangles, Fig. 3b,d,f and supplementary material for comparison). The 5–15 Hz frequency band is the most relevant frequency band to investigate magma migration, since a high amount of energy is radiated by volcano-tectonic (i.e., brittle failure) earthquakes in this frequency range (Lahr et al., 1994).

Data were pre-processed using MSNoise software (Lecocq et al., 2014) and we then adapted the steps described in Taisne et al. (2011). The raw data are detrended and cosine tapered (10%) before being resampled from 128 to 40 Hz. The resulting trace is filtered between 5 and 15 Hz and the envelope is calculated. Finally, the data are decimated to 1 s (using the median).

The results are smoothed using a 5 and a 360 minutes rolling median before computing the seismic ratios. We only plot the values which are above the median of the background noise at both stations.

Please cite this article as: Caudron, C., et al., Magma migration at the onset of the 2012–13 Tolbachik eruption revealed by Seismic Amplitude Ratio Analysis, J. Volcanol. Geotherm. Res. (2015), http://dx.doi.org/10.1016/j.jvolgeores.2015.09.010

$$\frac{A_1}{A_2} = \frac{A_2^{cor}}{A_1^{cor}} exp(-B(r_1 - r_2)) \left(\frac{r_2}{r_1}\right)^n \quad (1)$$

with,

$$B = \frac{\pi f}{Q\beta} \quad (2)$$

where A is the amplitude at stations 1 and 2, A^{cor} is the corrected amplitude at stations 1 and 2, r is the distance between the source and stations 1 and 2 and $n = 1$ for body waves and $n = 0.5$ for surface waves. β is shear wave velocity (1000 m/s), Q is the quality factor for attenuation and f is the central frequency (10 Hz).

We use the natural logarithm (ln) of the data to present and discuss the results:

$$ln\frac{A_1}{A_2} = ln\frac{A_2^{cor}}{A_1^{cor}} - (B(r_1 - r_2)) + n\,ln\left(\frac{r_2}{r_1}\right). \quad (3)$$

Site effect, gain and sensitivity changes will correspond to a vertical shift in a natural logarithm plot, whereas any change in attenuation and wave regime will coincide with a dilation or contraction. We can therefore discuss the relative changes rather than the actual values that would require further corrections (e.g. site effects). Each station pair shows a clear fluctuation starting between 26 and 27 November (Fig. 4). By inspecting in details the amplitude ratio around the 27 November (Fig. 5), the first significant variation is detected as early as 14:00 UTC on 26 November. This timing is coincident with a swarm of shallow volcanic earthquakes in Plosky Tolbachik area (Fig. 2). The increase in ratio proceeded in different phases and culminated at ~05:40 UTC on 27 November (Fig. 5). It then decreased for a short time at KMN/BMZ and KMN/LGN before re-increasing and finally stabilizing around 10:00 UTC, while a return to pre-crisis levels is noted at BZM/LGN after 05:40 UTC. We note that this sequence can be sub-divided into several sections which show the complexity of the dynamics.

Between 27 and 28 November, another important fluctuation in the amplitude ratios is detected at pairs including KMN station (Fig. 5). It starts around 17:00 UTC on 28 November and ends around 02:00 UTC on 29 November.

5. Discussion

Temporal changes in the amplitude ratio can be attributed to either a change in the attenuation law or a change in the source–receiver distance. A variation of the attenuation at this time-scale is unlikely. Hence, the change in the ratio likely corresponds to a change in the source locations.

The use of this simple technique provides important results. Fig. 5 shows that significantly changing energy is recorded by the network nearly a day before the eruption (starting on 26 November, for ~20 hours). The time evolution of this seismicity could be related to a change in the source location. The most energetic phase occurred at 05:00 UTC on 27 November coincident with a swarm of VTs. Seismic waveforms for this swarm are relatively more saturated at BZM and BZG (Fig. 3a and

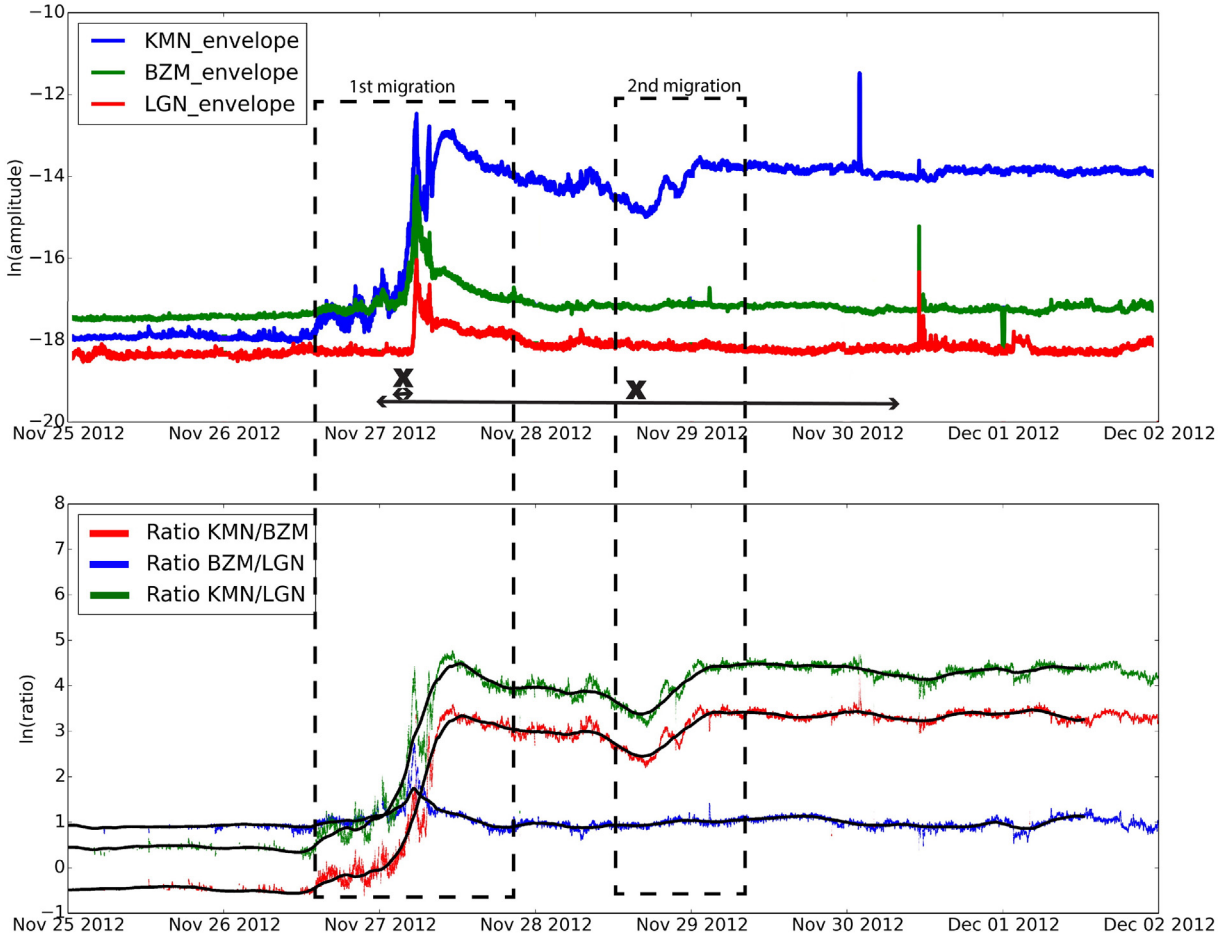

Fig. 4. Seismic intensity ratios: Upper: Seismic envelope calculated every second at BZM, KMN, and LGN in the 5–15 Hz frequency band (5-min rolling median). Lower: Intensity ratio computed every second after a smoothing using a 6-hr rolling median (black solid line) and 5-min rolling median (colored lines). We only plot the ratios having a seismic envelope (after smoothing) above the 50th percentile of the background noise. Important periods are highlighted using black rectangles. Periods of clipped data are indicated using black crosses (longer and shorter periods correspond to KMN and BZM, respectively). (For interpretation of the references to color in this figure legend, the reader is referred to the web version of this article.)

Please cite this article as: Caudron, C., et al., Magma migration at the onset of the 2012–13 Tolbachik eruption revealed by Seismic Amplitude Ratio Analysis, J. Volcanol. Geotherm. Res. (2015), http://dx.doi.org/10.1016/j.jvolgeores.2015.09.010

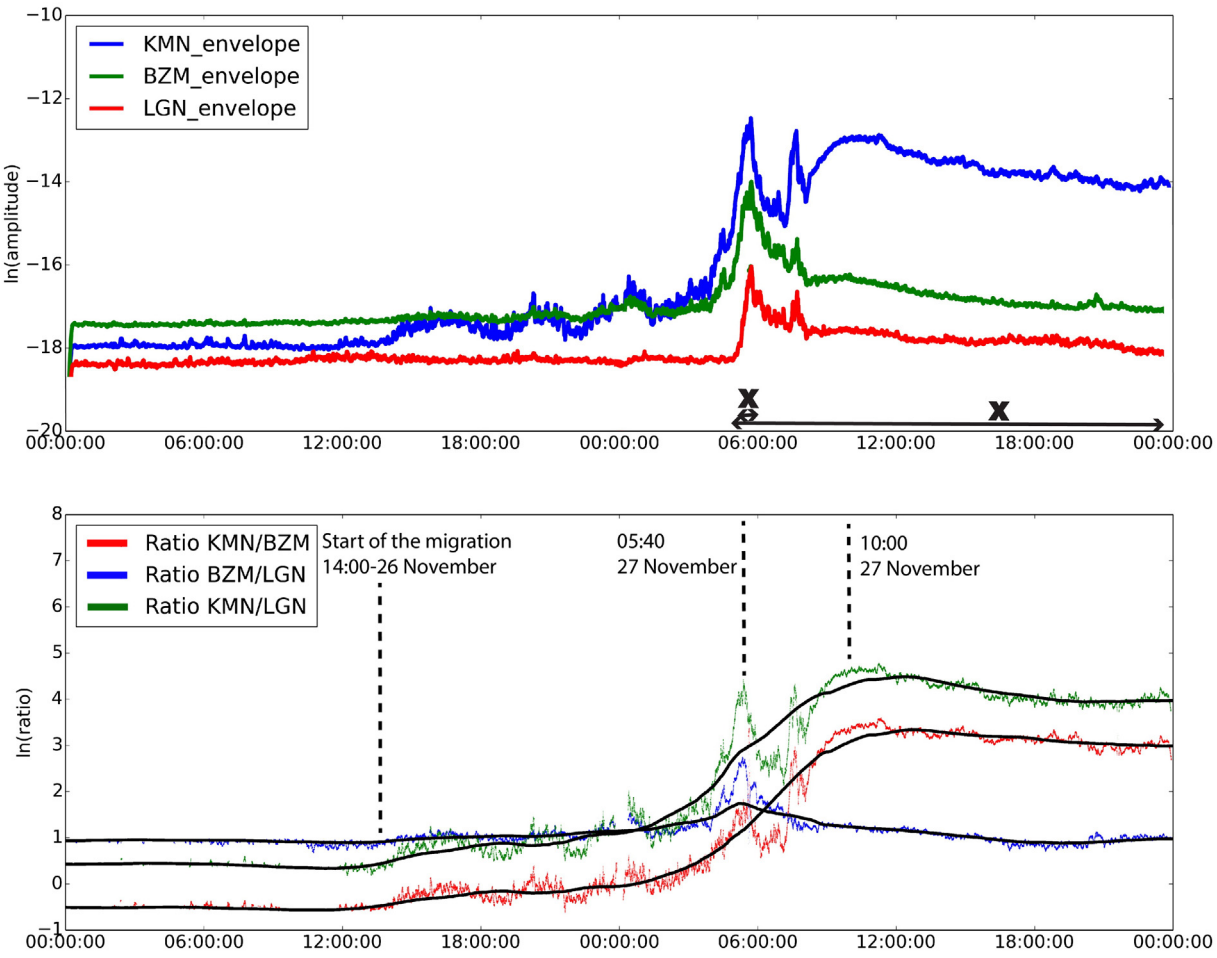

Fig. 5. Seismic intensity ratios: zoom: Upper: Seismic envelope computed every second at BZM, KMN, and LGN in the 5–15 Hz frequency band (5-min rolling median). Lower: Intensity ratio calculated every second after a smoothing using a 6-hr rolling median (black solid line) and 5-min rolling median (colored lines). We only plot the ratios having a seismic envelope (after smoothing) above the 50th percentile of the background noise. Important periods are highlighted using dashed lines. Periods of clipped data are indicated using black crosses (longer and shorter periods correspond to KMN and BZM, respectively). (For interpretation of the references to color in this figure legend, the reader is referred to the web version of this article.)

supplementary material, respectively) and show more impulsive P and S wave arrivals than elsewhere. After 06:00 UTC, the ratio decreased at BZM–LGN, but re-increased at KMN–BZM and KMN–LGN and reached a maximum when the eruptive tremor, corresponding to lava flows, was recorded (07:30–10:00 UTC). Two groups of vents were observed the next morning.

In order to capture the main characteristics of the stress migration, we will use a 6 hours sliding median filter to smooth the short term variations (Fig. 5) and compare the results to the calculated intensity ratios. Knowing the distance and assuming reasonable values for the attenuation law ($Q = 125$, $n = 1$), we can compute the theoretical ratios between 2 stations in a 2-D cross section. Comparison is therefore possible assuming a migration within a vertical plan defined by the stations LGN, BZM and KMN (Fig. 1). This hypothesis is supported by the observed seismicity and the alignment of the 2 eruptive vents. Fig. 6 shows that the trend of the ratios between the stations does not depend on the attenuation law but only on the change in source location. The amplitude of this change is affected, but we will only qualitatively discuss the results. It is worth noting that at high frequency seismicity, the radiation pattern becomes rapidly isotropic (e.g., (Takemura et al., 2009)). Besides, we look at the seismic energy most likely released from randomly oriented micro-cracks.

We are now discussing the time evolution and the trend of the changes rather than the actual values; i.e., any correcting factors, gain, sensitivity and site effect will only shift the curves up or down in the ln scale. For both ratios involving KMN, the observations suggest that the seismicity migrates toward this station (Fig. 5) which is consistent with the eruption location (Fig. 2). More interestingly, the ratio BZM/LGN displays relatively constant values except from 14:00 November 26 to 05:40 November 27, where the ratio increased then decreased back to its initial values (Fig. 5). Since we know the location of the eruption, we can assess the possible pathways for this magma propagation. The black arrows drawn on Fig. 7c indicate several different possibilities which are qualitatively in agreement with the theoretical ratios (Fig. 7a,b). The probable magma propagation implies a vertical migration between BZM and KMN (increasing part of the ratio BZM/LGN, Fig. 5) followed by a more lateral migration (decreasing part of the ratio BZM/LGN, Fig. 5) toward the eruptive vents (black arrows, Fig. 7c).

The second episode of migration between 17:00 UTC on 28 November and ~02:00 UTC on 29 November occurred when a seismic swarm started with a M = 2.6 earthquake at a distance of 16–20 km to the south from Plosky Tolbachik on November 28, 2012 at 20:31 UTC (Fig. 2). This did not lead to an eruption. The maximum in swarm activity occurred on November 30 with earthquakes of M = 5.4, M = 4.1 and M = 4.6 and about 30 of M = 2–3 located between 0–10 km of depth below sea level. The seismicity then decreased until December 5–6. The main M = 5.4 earthquake was one of the five largest seismic events ever detected by the regional seismic network in the Kyuchevskoy volcano

Please cite this article as: Caudron, C., et al., Magma migration at the onset of the 2012–13 Tolbachik eruption revealed by Seismic Amplitude Ratio Analysis, J. Volcanol. Geotherm. Res. (2015), http://dx.doi.org/10.1016/j.jvolgeores.2015.09.010

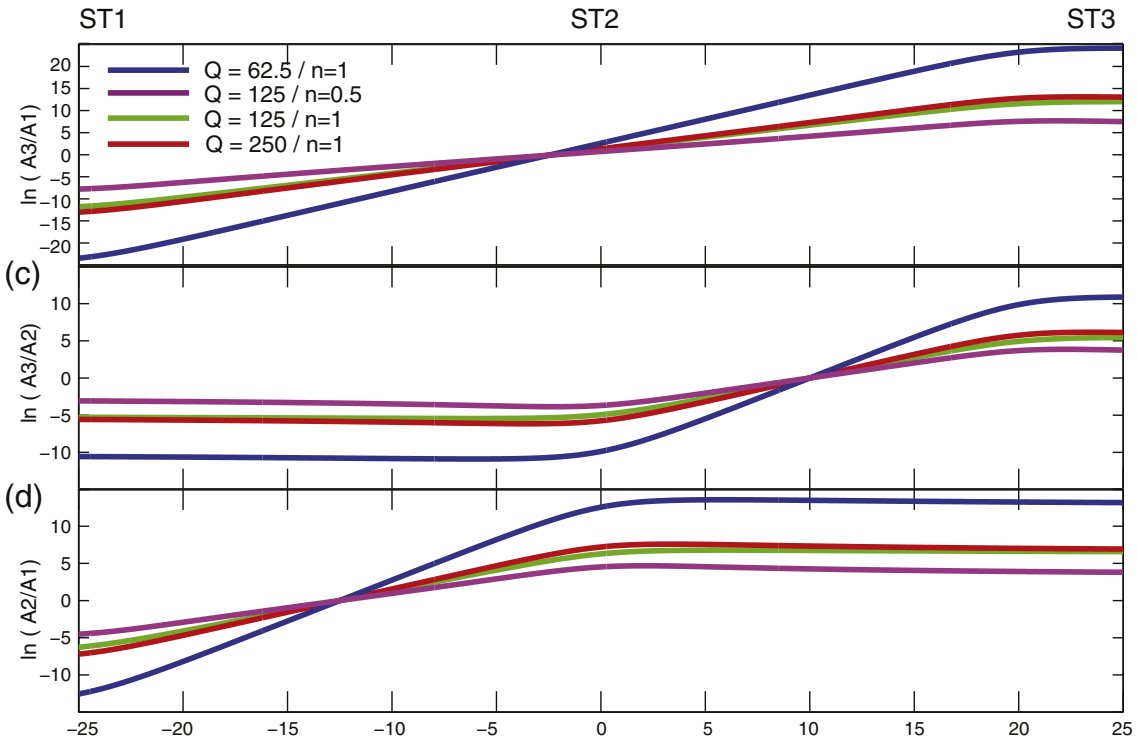

Fig. 6. Theoretical ratios: Theoretical ratios between different station pairs, for different Q and n values, for a horizontal migration taking place at 4 km of depth. ST1, ST2, and ST3 are the stations and A is the amplitude.

group region for the period ranging between 1962–2012. The energy of this seismic swarm is nearly 50 times more than the energy of all earthquakes at Plosky Tolbachik and the 2012–13 Tolbachik eruption. This seismic swarm is very similar to seismicity recorded in 1975 preceding the 1975–76 Tolbachik eruption, and, therefore, can be regarded as a possible failed eruption. Since the amplitude only increased at KMN and the signal is dominated by the ongoing eruption, it is difficult to better constrain the origin of this activity. The seismic data are indeed saturated after the onset of the eruption at KMN (Fig. 3c) which underestimates the seismic energy recorded at this station. To assess the effect of clipped data on the amplitude ratios, we computed the percentage of saturated values within a given time window (e.g., 30 s). This revealed that less than 40% of the window length is saturated, in the worst case for KMN, while it does not exceed 5% for BZM. The results are similar when taking different time windows. Therefore, the median is not affected the saturation. We note that the migration started before the seismic data became clipped.

Overall, the derived information is very important in such remote areas. The significant variation occurs when the seismic event activity becomes intense. From a real-time monitoring perspective, locating each event would be extremely difficult and time consuming. Therefore, by using simple continuous analysis based on ratios of seismic intensity, a rapid diagnosis can be drawn which can support monitoring efforts and volcanic activity evaluation.

6. Conclusions

In contrast to the 1975–76 Tolbachik eruption, the 2012–13 Tolbachik eruption was preceded by only weak precursory activity. The amplitude ratio analysis allows the detection of the main phases of migration

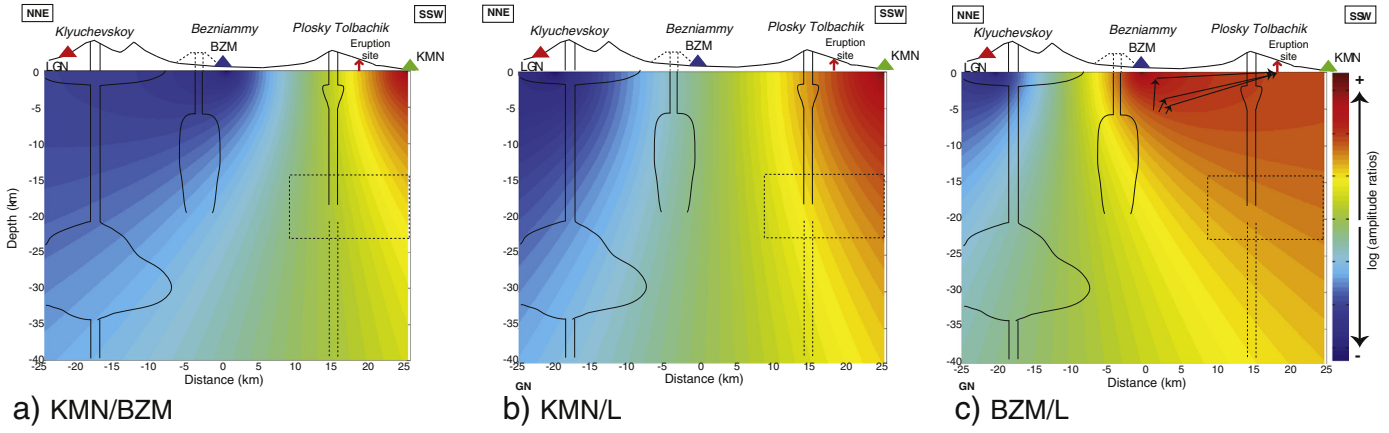

Fig. 7. Imaging migration: Theoretical ratios between 2 stations in a 2-D cross section along the line in Fig. 1. (a) Ln(KMN/BZM) (b) Ln(KMN/LGN) (c) Ln(BZM/LGN), for $n = 1$ and $Q = 125$. Storage regions are from Fedotov et al. (2011) and dashed arrows indicate the possible links between them. The black arrows on (c) depict the probable magma propagation based on the observed ratios.

Please cite this article as: Caudron, C., et al., Magma migration at the onset of the 2012–13 Tolbachik eruption revealed by Seismic Amplitude Ratio Analysis, J. Volcanol. Geotherm. Res. (2015), http://dx.doi.org/10.1016/j.jvolgeores.2015.09.010

which are well correlated with the main episodes using evidence from other analyses (Melnikov & Volynets, 2015 in this issue). A seismic migration started ~20 hours before the suspected eruption. The migration proceeded in several stages and reveals a vertical migration ~5 km under the northern slope of Plosky Tolbachik volcano potentially interacting at shallower depths with an intermediate region, initiating a sub-lateral migration, and leading to the eruption. Our results show the potential of this technique to extract information even with a limited number of sensors, in this case thanks to their alignment. This analysis would be particularly useful for real-time monitoring in observatories, especially when the seismic event activity becomes too intense to locate individual seismic events.

Acknowledgments

Observations were carried out by Kamchatkan Branch of Geophysical Survey of Russian Academy of Sciences. This research was supported by Russian Foundation of Basic Research (project 13-05-00117).

This work comprises Earth Observatory of Singapore contribution no. 105. This research is supported by the National Research Foundation Singapore and the Singapore Ministry of Education under the Research Centres of Excellence initiative.

References

Belousov, A., Belousova, M., Edwards, B., Volynets, A., Melnikov, D., 2015. Overview of the precursors and dynamics of the 2012–13 basaltic fissure eruption of Tolbachik Volcano, Kamchatka, Russia. J. Volcanol. Geotherm, Res (in this issue).

Chebrov, V.N., Droznin, D.V., Kugaenko, Y.A., Levina, V.I., Senyukov, S.L., Sergeev, V.A., Shevchenko, Y.V., Yashchuk, V.V., 2013. The system of detailed seismological observations in Kamchatka in 2011. J. Volcanol. Seismol. 5 (3), 161–170.

Churikova, T., Gordeychik, B., Iwamori, H., Nakamura, H., Nishizawa, T., Haraguchi, S., Yasukawa, K., Ishizuka, O., 2015. Petrological and geochemical evolution of the Tolbachik volcanic massif, Kamchatka, Russia. J. Volcanol. Geotherm. Res. (in this issue).

Dvigalo, V., Svirid, I., Shevchenko, A., 2014. The first quantitative estimates of parameters for the Tolbachik Fissure Eruption of 2012–2013 from aerophotogrammetric observations. J. Volcanol. Seismol. 8 (5), 261–268.

Edwards, B., Belousov, Belousova, Volynets, A., Melnikov, D., Chirkov, S., Senyukov, S., 2013. Another Great Tolbachik eruption? Eos Trans AGU 94 (21), 189–191.

Fedotov, S.A., Markhinin, Y.K. (Eds.), 1983. The Great Tolbachik Fissure Eruption, 1975–1976. Cambridge University Press, New York (341 pp.).

Fedotov, S.A., Balesta, S.T., Masurenkov, Yu.P. (Eds.), 1991. Active Volcanoes of Kamchatka. Nauka, Moscow.

Fedotov, S., Utkin, I., Utkina, L., 2011. The peripheral magma chamber of Ploskii Tolbachik, a Kamchatka basaltic volcano: activity, location and depth, dimensions, and their changes based on magma discharge observations. J. Volcanol. Seismol. 5 (6), 369–385.

Kugaenko, Y., Saltykov, V., Titkov, N., 2015. New unrest of Plosky Tolbachik volcano in 2012 revealed by parameters of local seismicity and GPS data. J. Volcanol. Geotherm. Res. (in this issue).

Lahr, J., Chouet, B., Stephens, C., Power, J., Page, R., 1994. Earthquake classification, location, and error analysis in a volcanic environment: implications for the magmatic system of the 1989–1990 eruptions at Redoubt Volcano Alaska. J. Volcanol. Geotherm. Res. 62 (1), 137–151.

Lecocq, T., Caudron, C., Brenguier, F., 2014. MSNoise, a Python package for computing and monitoring seismic velocity changes using ambient noise. Seismol. Res. Lett. 85, 715–726.

Melnikov, D., Volynets, A., 2015. Remote sensing and petrological observations on the 2012–2013 fissure eruption at Tolbachik volcano, Kamchatka: implications for reconstruction of the eruption chronology. J. Volcanol. Geotherm, Res (in this issue).

Senyukov, S., 2006. Monitoring of volcanic activity in Kamchatka by Remote Sensing Techniques in 2000–2004. J. Volcanol. Seismol. 3, 68–78.

Taisne, B., Brenguier, F., Shapiro, N.M., Ferrazzini, V., 2011. Imaging the dynamics of magma propagation using radiated seismic intensity. Geophys. Res. Lett. 38 (4).

Takemura, S., Furumura, T., Saito, T., 2009. Distortion of the apparent S-wave radiation pattern in the high-frequency wavefield: Tottori-Ken Seibu, Japan, earthquake of 2000. Geophys. J. Int. 178 (2), 950–961.

Volynets, A., Melnikov, D., Yakushev, A., 2013. First data on composition of the volcanic rocks of the IVS 50th anniversary Fissure Tolbachik eruption (Kamchatka). Dokl. Earth Sci. 452 (1), 953–957. http://dx.doi.org/10.1134/S1028334X13090201.

Please cite this article as: Caudron, C., et al., Magma migration at the onset of the 2012–13 Tolbachik eruption revealed by Seismic Amplitude Ratio Analysis, J. Volcanol. Geotherm. Res. (2015), http://dx.doi.org/10.1016/j.jvolgeores.2015.09.010